

# Effect of surface charge self-organization on gate-induced 2D electron and hole systems

Vitaly A. Tkachenko<sup>1,2</sup>, Olga A. Tkachenko<sup>1</sup>, Dmitry G. Baksheev<sup>2</sup>, Oleg P. Sushkov<sup>3</sup>

*1 Rzhanov Institute of Semiconductor Physics, Siberian Branch, Russian Academy of Sciences, Akad. Lavrenteva Ave., 13, Novosibirsk, 630090, Russia*

*2 Novosibirsk State University, Pirogova Str., 1, Novosibirsk, 630090, Russia*

*3 University of New South Wales, Sydney, 2052, Australia*

Corresponding author: Vitaly A. Tkachenko (vtkach@isp.nsc.ru)

Received 26 March 2020 ♦ Accepted 21 August 2020 ♦ Published 30 September 2020

**Citation:** Tkachenko VA, Tkachenko OA, Baksheev DG, Sushkov OP (2020) Effect of surface charge self-organization on gate-induced 2D electron and hole systems. *Modern Electronic Materials* 6(3): 101–106. <https://doi.org/10.3897/j.moem.6.3.63361>

## Abstract

A simple model has been suggested for describing self-organization of localized charges and quantum scattering in undoped GaAs/AlGaAs structures with 2D electron or hole gas created by applying respective gate bias. It has been assumed that these metal / dielectric / undoped semiconductor structures exhibit predominant carrier scattering at localized surface charges which can be located at any point of the plane imitating the GaAs / dielectric interface. The suggested model considers all these surface charges and respective image charges in metallic gate as a closed thermostated system. Electrostatic self-organization in this system has been studied numerically for thermodynamic equilibrium states using the Metropolis algorithm over a wide temperature range. We show that at  $T > 100$  K a simple formula derived from the theory of single-component 2D plasma yields virtually the same behavior of structural factor at small wave numbers as the one given by the Metropolis algorithm. The scattering times of gate-induced carriers are described with formulas in which the structural factor characterizes frozen disorder in the system. The main contribution in these formulas is due to behavior of the structural factor at small wave numbers. Calculation using these formulas for the case of disorder corresponding to infinite  $T$  has yielded 2–3 times lower scattering times than experimentally obtained ones. We have found that the theory agrees with experiment at disorder freezing temperatures  $T \approx 1000$  K for 2D electron gas specimen and  $T \approx 700$  K for 2D hole gas specimen. These figures are the upper estimates of freezing temperature for test structures since the model ignores all the disorder factors except temperature.

## Keywords

undoped structures, gate-induced 2D systems, surface charge, disorder freezing temperature.

## 1. Introduction

Charging of surface and interface defects is one of the key physical phenomena in semiconductor electronics [1–4]. Little is known however about this phenomenon in undoped GaAs/AlGaAs structures. A study of these structures containing gate-induced 2D quantum electron or hole

systems has been initiated recently [5–12]. The situation with a thin gate dielectric and shallow location of gate-induced systems is of interest for studying the role of surface charges [11, 12] and for the development of quantum systems with ultimately small characteristic lateral sizes [13]. The aim of this work is to briefly describe the simple model [14] that we suggested for illustrating the effect of

electrostatic self-organization of surface charges on the gate-induced 2D electron or hole gas.

## 2. Test object and suggested model

In contrast to the standard modulation doping method, the 2D gas is in this case is created at low temperatures by bias  $V_g$  between the metallic gate and metallic contacts connected to the GaAs working layer [5–11]. The charge on the surface of the GaAs protective layer is generated in equilibrium at  $V_g = 0$  and a high temperature, along with the image charge in the metal, and a common Fermi level is established in the metal / dielectric / undoped semiconductor structure (Fig. 1a, b). The common  $E_F$  level is pinned by the defect states near the band gap center at the boundaries of the epitaxial heterostructure with the insulator and the GaAs semi-insulating substrate. This provides for flat bands in the semiconductor. In accordance with the Gauss theorem the  $\text{Al}_2\text{O}_3$  gate dielectric thickness  $d$  (20–30 nm) and the difference in the work functions  $A_e$  for the adjacent GaAs layer and the Ti gate

(Fig. 1b) determine the negative charge concentration  $n_\sigma$  at the GaAs protective layer and the positive charge concentration at the metal/dielectric interface:

$$n_\sigma = \epsilon_0 \epsilon_{\text{ins}} \frac{A_e}{ed} \quad (1)$$

Here  $\epsilon_0$  is the dielectric constant,  $\epsilon_{\text{ins}} \approx 8$  is the dielectric permeability of  $\text{Al}_2\text{O}_3$ ,  $A_e \approx 0.3$  eV, and  $e > 0$  is the elementary charge. Upon cooling the earthed gate structure to  $T \sim 1$  K its band diagram and the  $A_e$  and  $n_\sigma$  parameters remain the same as in equilibrium. The concentration  $n_\sigma \sim 5 \cdot 10^{11} \text{ cm}^{-2}$  is assumed to be constant even if  $V_g \neq 0$  and 2D gas is formed at a low temperature (Fig. 1c, d). In this case the bands of the layers 2, 3 and 4 in Fig. 1d are no longer flat.

Equation (1) describes the area-average concentration of charges trapped by point defects (traps) at  $V_g = 0$  and a sufficiently high temperature on the surface of the GaAs protective layer. The distribution of the surface charges does not change below some “freezing temperature”. This temperature is determined by the energy of electron transition to the leakage level from the deep traps, but this freezing temperature is not known for undoped structures.

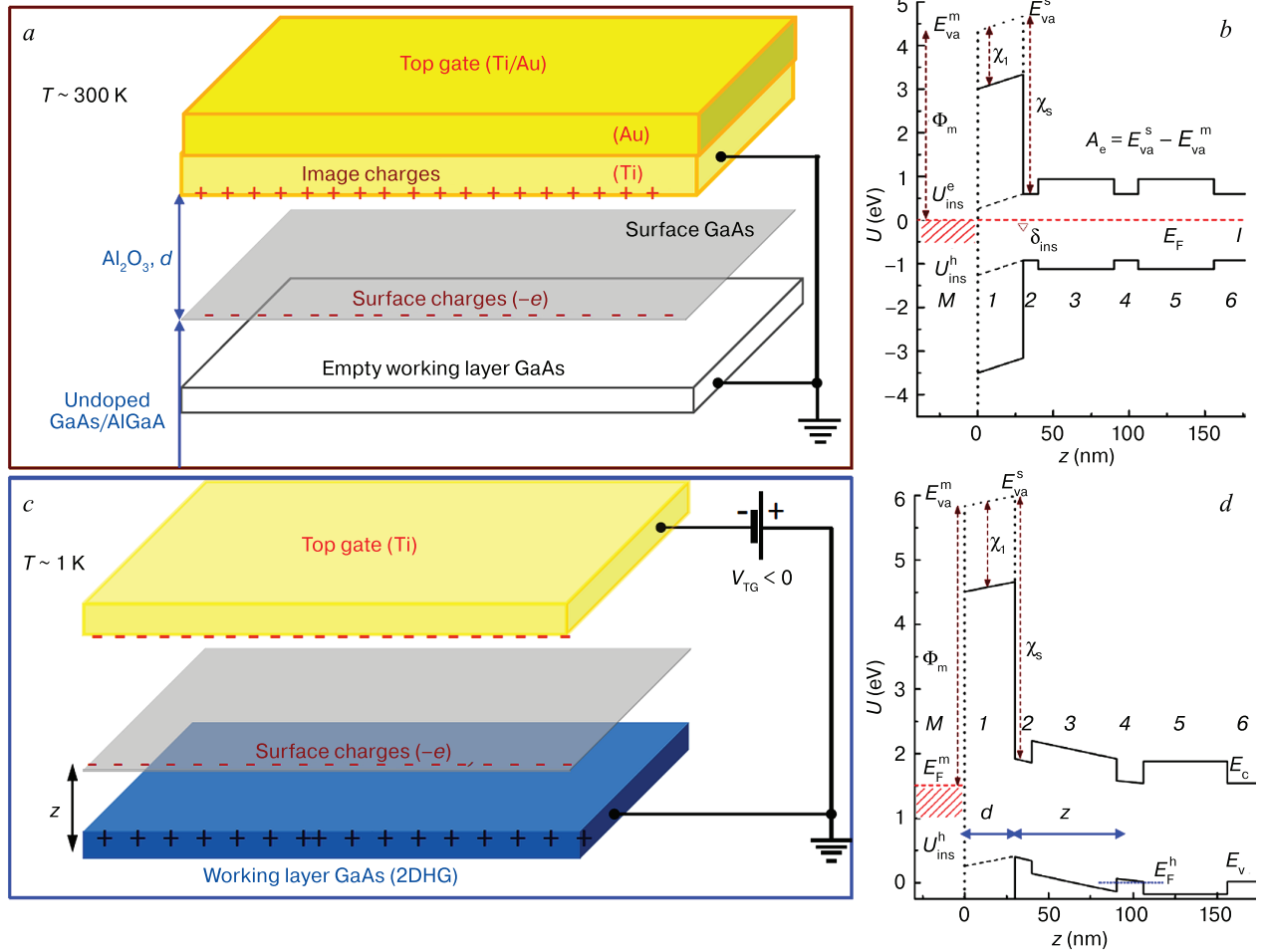


**Figure 1.** Schematic images of the object of study: (a, b) metal-dielectric-undoped semiconductor structure and band diagram in thermodynamic equilibrium:  $M$  – metal (Ti),  $I$  –  $\text{Al}_2\text{O}_3$ , 2, 4, 6 – GaAs, 3, 5 – AlGaAs,  $\Phi_m$  – work function of Ti,  $\chi_1$ ,  $\chi_s$  – electron affinity of  $\text{Al}_2\text{O}_3$  and GaAs, working layer 4 is empty; (c, d) a variant of the operating mode corresponding to a 2DHG ( $T \sim 1$  K,  $eV_{\text{TG}} < 0$  is the difference of the Fermi levels in the working layer and the upper gate).

Frozen disorder in the locations of surface charges and hence image charges in the metal, together produce static fluctuations of electrostatic potential at which mobile carriers are scattered in 2D gas at  $\sim 1$  K if the gas is located close to the surface ( $z = 30\text{--}60$  nm) [11, 12].

We simulate this disorder and calculate carrier scattering times in 2D gas within a simple model [14]. This model ignores the difference in the binding energies of electrons and GaAs surface traps (i.e., they are considered chemically equivalent [4]). It is taken into account that the point trap concentration on the GaAs surface is very high ( $\sim 10^{13}$  cm $^{-2}$  [1, 4]) in comparison with  $n_\sigma$ . It is assumed that electron exchange between adjacent traps in thermodynamic equilibrium on the surface is much more intense than between the surface, the gate and the semiconductor bulk. It is accepted for simplicity that point charges can be trapped at any point of the ideal plane imitating the real GaAs/Al $_2$ O $_3$  interface.

The state distribution of this thermostated system of charges with a fixed number of particles obeys canonical Gibbs distribution and the system in thermodynamic equilibrium is similar to classic single-component 2D plasma [15, 16]. In the suggested model all the disorder factors except the equilibrium temperature are disregarded, and the disorder itself and its effect on the scattering times in 2D gas can be analytically described.

### 3. Basic definitions and final formulas of the model

The point surface charge distribution determined by the radius vectors  $\mathbf{r}_i = (x_i, y_i)$  can be conveniently described with a Fourier transform:

$$\rho_q = \sum_i e^{i\mathbf{q}\mathbf{r}_i}. \tag{2}$$

We assume that the number of charges  $N$  and the system area  $A$  tend to infinity and the disorder at  $\rho_q$  is *isotropic*:

$$|\rho_q|^2 = Nn_\sigma (2\pi)^2 \delta(\mathbf{q}) + |\tilde{\rho}_q|^2, |\tilde{\rho}_q|^2 = n_\sigma A \times F_q. \tag{3}$$

In the solution of Poisson’s equation the delta function term yields a constant potential that can be neglected. Of interest are only the fluctuations of potential caused by the isotropic structural factor  $F_q$ . Given mutually independent and completely random  $\mathbf{r}_i$  we have  $F_q = 1$ , and then Eq. (3) describes white noise.  $\sigma$

Deviations of  $F_q$  from 1 due to Coulomb’s charge interaction can be taken into account within the theory of weakly non-ideal single-component 2D plasma [15, 16]. A critical point in analyzing any plasma of this type is to choose the method of maintaining electrical neutrality of the system. As a rule, this is achieved by formally introducing a homogeneous background neutralizing charge into the ultrathin layer that is occupied by the single-component plasma [15–18]. On the contrary electrical neutrality in the case considered at the zero gate voltage is provided by the

image charge in the metal (Ti/Au) for each point charge on the semiconductor surface. Temperature  $T$  is another theory parameter along with  $n_\sigma$ . The following simple formula has been derived within the case-adapted theory:

$$F_q = \left[ 1 - \frac{\tilde{k}_T}{q + \tilde{k}_T} \right]. \tag{4}$$

Here  $\tilde{k}_T = k_T C_d$ ,  $k_T = \frac{2\pi e^2 n_\sigma}{\epsilon T}$ ,  $C_d = \frac{1 - \exp(-2qd)}{1 - \lambda \exp(-2qd)}$ ,  $\epsilon = \frac{\epsilon_1 + \epsilon_2}{2}$ ,  $\lambda = \frac{\epsilon_1 - \epsilon_2}{\epsilon_1 + \epsilon_2}$ ,  $\epsilon_1 = \epsilon_{\text{GaAs}}$ ,  $\epsilon_2 = \epsilon_{\text{ins}}$ . When deriving Eq. (4) we

ignored the difference in the dielectric permeabilities of the GaAs and AlGaAs layers and by analogy with an earlier work [20] took into account the image charges in the metallic gate.

Note that for standard structures formed by remote doping, a theory was developed long time ago describing the effect of ultrathin charged impurity layers on the low-temperature parameters of high-mobility 2D carriers [17–19]. This theory is based on the knowledge of isotropic  $F_q$  for the charged impurity distribution in the delta layer. For the undoped structures in question we developed a similar theory. In this theory the quantum ( $\tau_q$ ) and transport ( $\tau_t$ ) carrier scattering times in 2D gas can be expressed with the following formulas:

$$\begin{aligned} \tau_q^{-1} &= \frac{\pi n_\sigma}{2m^*} I_q, \quad I_q = \frac{2}{p_F} \int_0^\infty \frac{F_q}{\left(\frac{q}{k} + D_z\right)^2} e^{-2qz} C_d^2 dq; \\ \tau_t^{-1} &= \frac{\pi n_\sigma}{2m^*} I_t, \quad I_t = \frac{2}{p_F^3} \int_0^\infty \frac{F_q}{\left(\frac{q}{k} + D_z\right)^2} e^{-2qz} C_d^2 q^2 dq; \tag{5} \\ k &= \frac{2m^* e^2}{\epsilon}, \quad D_z = 1 + e^{-2qz} \frac{\lambda - \exp(-2qd)}{1 - \lambda \exp(-2qd)}. \end{aligned}$$

Here  $p_F$  is the Fermi momentum in the 2D gas, and  $F_q$  is given by Eq. (3) for  $\mathbf{r}_i$  distributions frozen at some unknown equilibrium temperature. Note that Eqs. (5) follow from Poisson’s equation with account of gate screening and self-screening of carriers in the 2D gas in the Thomas–Fermi approximation and from Fermi’s golden rule where the interaction matrix element is found from unperturbed carrier wave functions in the 2D gas.

Figure 2 shows an example of the behavior of the integrand terms in Eqs. (5) for  $\tau_q$  and  $\tau_t$  with  $F_q$  determined by the adapted single-component plasma theory (Eq. (4)). Evidently, it is sufficient to calculate the integrals in Eqs. (5) for the  $0 < q < 0.1$  nm $^{-1}$  range and substitute the dielectric permeabilities of Al $_2$ O $_3$  and GaAs with their average.

### 4. Metropolis algorithm calculations

For thermostated systems with a constant number of interacting particles, a universal, efficient and powerful modi-

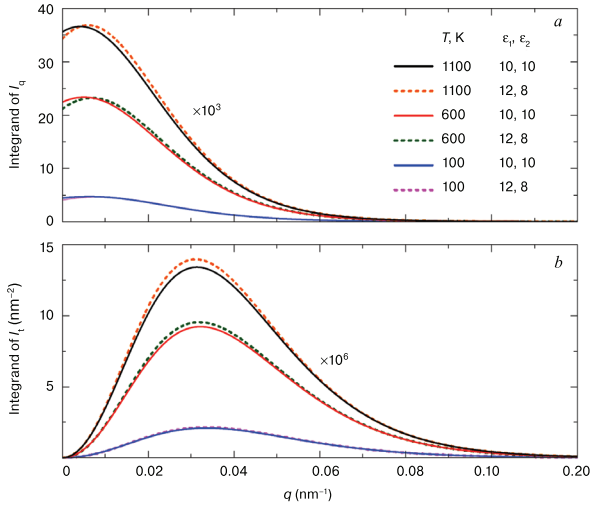


**Figure 2.** The behavior of the integrands in formulas (5) for the indicated  $T$  and structure with a 2DEG in which  $d = 25$  nm,  $z = 45$  nm,  $n_c = 5 \cdot 10^{11}$  cm $^{-2}$ .

fication of the Monte-Carlo method has existed for a long time, i.e., the Metropolis algorithm [21–24] providing a numerical solution of a key problem of statistical physics. The algorithm locates the maximum of the internal energy distribution  $W(E)$  for a system at a preset temperature, i.e., the most probable  $E$ , as well as the respective distributions of interacting particles  $r_i$ . Noteworthy this algorithm uses data on  $r_i$  and the internal energy of the system, i.e., it does not require calculating the system’s entropy and free energy. The calculated ratio of the probabilities of the system being in the two different states obeys the canonical Gibbs distribution [24]. Calculations with this algorithm were the main tool used for numerical simulation of single-component 2D plasma [16]. The original algorithm simulated systems of relatively heavy particles, and  $E$  calculations ignored the kinetic energy contribution [21, 22]. In the case considered this contribution can also be neglected because we deal with localized charges which are located for a long time in presumably equivalent chemical traps and change their coordinates quite rarely by jumps. In the suggested simple model for a system of point surface charges  $q_0$  located in the ideal plane and having respective image charges in the metal, equilibrium states may exist at arbitrarily low  $T$ .

We found these states numerically using the Metropolis algorithm and simultaneously observed the formation of a 2D Wigner crystal and its melting at  $T \sim 1$  K [16]. At  $T > 5$  K the structural factor  $F_q$  depends only on the absolute value  $q$  of the wave vector  $\mathbf{q}$ . The total simulated area was  $A > 2 \times 2 \mu\text{m}^2$  and contained up to  $N = n_c A = 60,000$  point charges ( $n_c \sim 5 \times 10^{11}$  cm $^{-2}$ ).

Taking into account the image charges in the gate the total system energy is the sum of pairwise interactions between vertical dipoles having the length  $2d$ :

$$U_{ij} = \frac{1}{2} \frac{q_0^2}{2\pi\epsilon\epsilon_0} \left[ r_{ij}^{-1} - \left( r_{ij}^2 + 4d^2 \right)^{-\frac{1}{2}} \right],$$

$$E = \frac{1}{2} \sum_{i \neq j} U_{ij}. \quad (6)$$

The multiplier  $1/2$  in  $U_{ij}$  takes into account the difference between the image charge and the real charge. We convoluted the simulated area into a torus and took the shortest distances  $r_{ij}$  on the torus for  $U_{ij}$  calculation. The kinetic energy of the charges was neglected. For each charge  $q_i$  we set a displacement in an arbitrary direction through a random distance which was not greater than the average distance between the charges and then recalculated the total system energy. If the energy decreased ( $\Delta E < 0$ ) the new location of the charge  $q_i$  was accepted, whereas for  $\Delta E \geq 0$  the new charge location was accepted only if

$\frac{\Delta E}{T} \geq r$  where  $r$  is a random value between 0 and 1. The iterations were continued after reaching a “constant”  $E$ . Due to the finiteness of  $N$  the relative width  $\delta E/E$  of the system’s internal energy distribution is not infinitely small:  $\delta E/E \sim 1/N^{1/2} \sim 0.01$ . For each  $E$  fluctuating near the most probable value, we found the  $r_i$  distributions and calculated  $\rho_q$ ,  $|\rho_q|^2$  using Eqs. (2) and (3). Then we found the mean  $|\rho_q|^2$  distribution for multiple iterations. This allowed us to imitate  $|\rho_q|^2$  for a far greater system than the test area. Example of this mean  $|\rho_q|^2$  distribution is shown in Fig. 3a. The white wide-centered cross is caused by a finite size of the calculation area in the  $(x, y)$  plane. The structural factor has no angular dependence outside this cross. By processing the  $|\rho_q|^2$  distribution we found the dependence of the structural factor on the absolute value of the wave number  $F_q$  (Fig. 3b). It can be seen from Fig. 3 that the  $F(q)$  dependences simulated using the Monte Carlo method are close to the theoretical ones (Eq. (4)) at  $q < 0.1$  nm $^{-1}$  and  $100 \text{ K} \leq T \leq 1100 \text{ K}$ . The considerable decrease in  $F(q)$  in comparison with that for white noise  $F_q = 1$  demonstrates the electrostatic self-organization of surface charge within the suggested simple model.

## 5. Comparison: calculation vs experiment

Our colleagues from the University of New South Wales, Australia, experimentally studied structures with gate-induced 2D electron gas ( $d = 25$  nm,  $z = 45$  nm) and 2D hole gas ( $d = 20$  nm,  $z = 68$  nm). We compared the scattering times  $\tau_q$  and  $\tau_t$  calculated using Eqs. (4) and (5) and the experimental scattering times for these specimens. The experimental scattering times (lifetimes) were estimated using a standard method [25–28]. The transport scattering time  $\tau_t$  in the experiment was determined from the carrier mobility  $\mu$ , and the quantum time  $\tau_q$  was found from the measured magnetic field dependences of the Shubnikov–de Haas oscillations amplitude. The parameter in these cases was the experimental density of the gate-induced 2D gas, i.e., the Fermi momentum in Eqs. (5). The data and details of their processing for obtaining experimental  $\tau_q$  will be published separately. This work focuses on the key simulation results. For the typical densities of 2D electron gas ( $n_c \sim 1.4 \times 10^{11}$  cm $^{-2}$ )

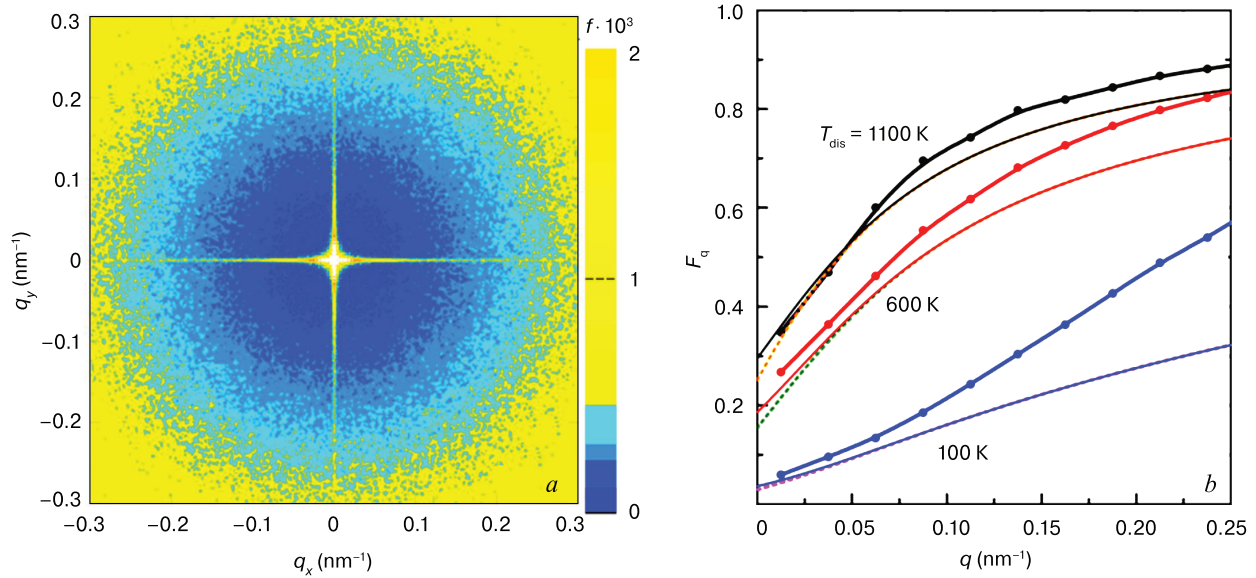


**Figure 3.** (a) An example of the averaged distribution  $|\rho_q|^2$  in the case of  $n_\sigma = 5 \cdot 10^{11} \text{ cm}^{-2}$  in an equilibrium state with a temperature  $T = 100 \text{ K}$ : Monte Carlo calculation; (b) dependence of the isotropic structural factor  $F_q$  for the same  $n_\sigma$  and indicated  $T$ . Thick solid lines were obtained by the Monte Carlo method. Thin solid and dotted lines are calculated according to the theory of a one-component plasma.

and 2D hole gas ( $n_h \sim 0.6 \times 10^{11} \text{ cm}^{-2}$ ) the experimental  $\tau_t$  were 2–3 times greater than those calculated in the assumption of a fully disordered surface charge distribution ( $F_q = 1$ ) which corresponds to the infinite temperature  $T$  in this model. The experimental quantum scattering time  $\tau_q$  also was greater than that calculated in the  $F_q = 1$  assumption. The underestimation of the theoretical scattering times  $\tau_{\text{theor}}$  in comparison with the experimental ones  $\tau_{\text{exp}}$  cannot be eliminated by making the natural assumption that experimental results are affected by theory-unaccounted scattering mechanisms with the characteristic time  $\tau_0$ . Indeed taking these mechanisms into account in the theory would further underestimate the calculated times ( $\tau_{\text{new}} < \tau_{\text{theor}} < \tau_{\text{exp}}$ ) in accordance with the common rule:

$$\frac{1}{\tau_{\text{new}}} = \frac{1}{\tau_{\text{theor}}} + \frac{1}{\tau_0}. \quad (7)$$

On the contrary, it is clear from Eqs. (5) that the self-organization of surface charges reduces  $F(q)$  (Fig. 3b) while increasing the carrier scattering times in 2D gas in comparison with the  $F_q = 1$  case. At  $F_q \neq 1$  Eqs. (4) and (5) contain only one free parameter, i.e., the  $\mathbf{r}_i$  distribution freezing temperature  $T$ . Restricting oneself to a single free parameter is quite convenient for finding the frozen  $F(q)$  by fitting the model to experiment at the characteristic 2D gas density. This fitting yielded disorder freezing times  $T \approx 1000 \text{ K}$  for a 2D electron gas specimen and  $T \approx 700 \text{ K}$  for a 2D hole gas specimen. Successful fitting indicates surface charge self-organization in the test structures. Since the simplified model disregards all the disorder factors except the thermodynamic equilibrium temperature, the resultant temperatures  $T$  are the upper estimates of the real disorder freezing temperature which

is unknown for this type of systems. However the  $\mathbf{r}_i$  disorder corresponding to the resultant temperatures  $T$  is probably close to the actually frozen one. It should also be noted that the simulated freezing temperatures of localized charges are almost two times higher than the actual temperatures of post-growth dielectric and gate deposition operations [5–12].

## 6. Conclusions

Summing up we considered self-organization of localized charges at the interface between gate dielectric and undoped semiconductor heterostructure containing gate-induced 2D electron or hole gas. In the suggested analytical formulas and Monte-Carlo calculations we used *only one* free parameter, i.e., the disorder freezing temperature. This temperature was found by comparing the calculated and experimentally measured transport and quantum scattering times for 2D carriers.

## Acknowledgements

This work was supported by Grant No. 19-72-30023 of the Russian Research Foundation. The calculations were carried out using computing resources of the Joint Supercomputer Center of the Russian Academy of Sciences under State Assignment No. 0306-2019-0011. We are grateful to colleagues A.R. Hamilton, O. Klochan and D.Q. Wang from the University of New South Wales, Australia, for the opportunity to compare calculations and theory with experimental data.

## References

- Cowley A.M., Sze S.M. Surface states and barrier height of metal-semiconductor systems. *J. Appl. Phys.*, 1965; 36(10): 3212–3220. <https://doi.org/10.1063/1.1702952>
- Sze S.M. Physics of semiconductor devices. New York: John Wiley, 1981: 868.
- Spicer W.E., Lindau I., Skeath P., Su C.Y. Unified defect model and beyond. *J. Vac. Sci. Technol.*, 1980; 17(5): 1019–1027. <https://doi.org/10.1116/1.570583>
- Darling R.B. Defect-state occupation, Fermi-level pinning, and illumination effects on free semiconductor surfaces. *Phys. Rev. B*, 1991; 43(5): 4071–4083. <https://doi.org/10.1103/PhysRevB.43.4071>
- Harrell R.H., Pyshkin K.S., Simmons M.Y., Ritchie D.A., Ford C.J.B., Jones G.A.C., Pepper M. Fabrication of high-quality one- and two-dimensional electron gases in undoped GaAs/AlGaAs heterostructures. *Appl. Phys. Lett.*, 1999; 74(16): 2328–2330. <https://doi.org/10.1063/1.123840>
- Tkachenko O.A., Tkachenko V.A., Baksheyev D.G., Pyshkin K.S., Harrell R.H., Linfield E.H., Ritchie D.A., Ford C.J.B. Electrostatic potential and quantum transport in a one-dimensional channel of an induced two-dimensional electron gas. *J. Appl. Phys.*, 2001; 89(9): 4993–5000. <https://doi.org/10.1063/1.1352024>
- Chen J.C.H., Wang D.Q., Klochan O., Micolich A.P., Das Gupta K., Sfigakis F., Ritchie D.A., Reuter D., Wieck A.D., Hamilton A.R. Fabrication and characterization of ambipolar devices on an undoped AlGaAs/GaAs heterostructure. *Appl. Phys. Lett.*, 2012; 100(5): 052101. <https://doi.org/10.1063/1.3673837>
- Chen J.C.H., Klochan O., Micolich A.P., Das Gupta K., Sfigakis F., Ritchie D.A., Trunov K., Reuter D., Wieck A.D., Hamilton A.R. Fabrication and characterisation of gallium arsenide ambipolar quantum point contacts. *Appl. Phys. Lett.*, 2015; 106(18): 183504. <https://doi.org/10.1063/1.4918934>
- Taneja D., Sfigakis F., Croxall A.F., Das Gupta K., Narayan V., Waldie J., Farrer I., Ritchie D.A. N-type ohmic contacts to undoped GaAs/AlGaAs quantum wells using only front-sided processing: application to ambipolar FETs. *Semicond. Sci. Technol.*, 2016; 31(6): 065013. <https://doi.org/10.1088/0268-1242/31/6/065013>
- Miserev D.S., Srinivasan A., Tkachenko O.A., Tkachenko V.A., Farrer I., Ritchie D.A., Hamilton A.R., Sushkov O.P. Mechanisms for strong anisotropy of In-plane g-factors in hole based quantum point contacts. *Phys. Rev. Lett.*, 2017; 119(11): 116803. <https://doi.org/10.1103/PhysRevLett.119.116803>
- Mak W.Y., Das Gupta K., Beere H.E., Farrer I., Sfigakis F., Ritchie D.A. Distinguishing impurity concentrations in GaAs and AlGaAs using very shallow undoped heterostructures. *Appl. Phys. Lett.*, 2010; 97(24): 242107. <https://doi.org/10.1063/1.3522651>
- Wang D.Q., Chen J.C.H., Klochan O., Das Gupta K., Reuter D., Wieck A.D., Ritchie D.A., Hamilton A.R. Influence of surface states on quantum and transport lifetimes in high-quality undoped heterostructures. *Phys. Rev. B*, 2013; 87(19): 195313. <https://doi.org/10.1103/PhysRevB.87.195313>
- Tkachenko O.A., Tkachenko V.A., Terekhov I.S., Sushkov O.P. Effects of Coulomb screening and disorder on an artificial graphene based on nanopatterned semiconductor. *2D Mater.*, 2015; 2(1): 014010. <https://doi.org/10.1088/2053-1583/2/1/014010>
- Tkachenko O.A., Baksheev D.G., Tkachenko V.A., Sushkov O.P. Modeling of localized charges self-organization at the boundary of a semiconductor with a gate dielectric. *Proceedings of the International Conference “Advanced Mathematics, Computations and Applications 2019” (AMCA-2019)*. Novosibirsk: NSU, 2019: 515–521 (In Russ.). <https://doi.org/10.24411/9999-016A-2019-10082>
- Fetter A.L. Electrodynamics and thermodynamics of a classical electron surface layer. *Phys. Rev. B*, 1974; 10(9): 3739–3745. <https://doi.org/10.1103/PhysRevB.10.3739>
- Gann R.C., Chakravarty S., Chester G.V. Monte Carlo simulation of the classical two-dimensional one-component plasma. *Phys. Rev. B*, 1979; 20(1): 326–344. <https://doi.org/10.1103/PhysRevB.20.326>
- Efros A.L., Pikus F.G., Samsonidze G.G. Maximum low-temperature mobility of two-dimensional electrons in heterojunctions with a thick spacer layer. *Phys. Rev. B*, 1990; 41(12): 8295–8301. <https://doi.org/10.1103/PhysRevB.41.8295>
- Das Sarma S., Hwang E.H., Kodyalam S., Pfeiffer L.N., West K.W. Transport in two-dimensional modulation-doped semiconductor structures. *Phys. Rev. B*, 2015; 91(20): 205304. <https://doi.org/10.1103/PhysRevB.91.205304>
- Das Sarma S., Stern F. Single-particle relaxation time versus scattering time in an impure electron gas. *Phys. Rev. B*, 1985; 32(12): 8442–8444. <https://doi.org/10.1103/PhysRevB.32.8442>
- Chaplik A.V. Possible crystallization of charge carriers in low-density inversion layers. *J. Experimental and Theoretical Physics*, 1972; 62(2): 395–398. URL: [http://www.jetp.ac.ru/cgi-bin/dn/e\\_035\\_02\\_0395.pdf](http://www.jetp.ac.ru/cgi-bin/dn/e_035_02_0395.pdf)
- Metropolis N., Rosenbluth A.W., Rosenbluth M.N., Teller A.H., Teller E. Equation of state calculations by fast computing machines. *J. Chem. Phys.*, 1953; 21(6): 1087. <https://doi.org/10.1063/1.1699114>
- Rosenbluth M.N., Rosenbluth A.W. Further results on Monte Carlo equations of state. *J. Chem. Phys.*, 1954; 22(5): 881. <https://doi.org/10.1063/1.1740207>
- Chib S., Greenberg E. Understanding the Metropolis-Hastings algorithm. *The American Statistician*, 1995; 49(4): 327–335. <https://doi.org/10.2307/2684568>
- Kotkin G.L. *Lectures on statistical physics*. Moscow; Izhevsk: Regulynaya i khaoticheskaya dinamika, 2006: 190. (In Russ.)
- Harrang J.P., Higgins R.J., Goodall R.K., Jay P.R., Laviron M., Delescluse P. Quantum and classical mobility determination of the dominant scattering mechanism in the two-dimensional electron gas of an AlGaAs/GaAs heterojunction. *Phys. Rev. B*, 1985; 32(12): 8126–8135. <https://doi.org/10.1103/PhysRevB.32.8126>
- Mani R.G., Anderson J.R. Study of the single-particle and transport lifetimes in GaAs/Al<sub>x</sub>Ga<sub>1-x</sub>As. *Phys. Rev. B*, 1988; 37(8): 4299–4302. <https://doi.org/10.1103/PhysRevB.37.4299>
- Coleridge P.T., Stoner R., Fletcher R. Low-field transport coefficients in GaAs/Ga<sub>1-x</sub>Al<sub>x</sub>As heterostructures. *Phys. Rev. B*, 1989; 39: 1120–1124. <https://doi.org/10.1103/PhysRevB.39.1120>
- Bystrov S.D., Kreshchuk A.M., Tuan L., Novikov S.V., Polyanskaya T.A., Savelev I.G., Shik A.Y. Shubnikov-de Hass oscillations in a nonuniform 2D electron-gas. *Semiconductors*, 1994; 28(1): 55–58.